Production of adsorbent for removal of propranolol hydrochloride: use of residues from *Bactris guineensis* fruit palm with economically exploitable potential from the Colombian Caribbean

Dison Stracke Pfingsten Franco[1], Jordana Georgin[1], Claudete Gindri Ramos[1], Matias S. Netto[2]; Brayan Lobo[1], Gabriel Jimenez[1], Eder C. Lima*[3,] , Farooq Sher[4],

[1-] *Universidad de la Costa, CUC, Barranquilla, Atlántico, Colombia.*

[2-] *Federal University of Santa Maria-UFSM, Santa Maria, RS, Brazil.*

[3-] *Federal University of Rio Grande do Sul, Porto Alegre, RS, Brazil.*

[4-] *Department of Engineering, Nottingham Trent University, Nottingham NG11 8NS, United Kingdom*

* profederlima@gmail.com

Abstract

The production and consequently the consumption of the pulp of the fruit of the palm tree *Bactris guineensis* occurs extensively in Colombia. The majority of the fruit is formed by waste (peel and core), producing high residual biomass. Thus, it is necessary to find a practical utilization of these peels, making the production and consumption of the fruit of the palm tree *Bactris guineensis* highly sustainable. This study produced activated biochar chemically activated using $ZnCl_2$ and utilized it as an effective adsorbent. The high micropollutant uptake is because of the high porosity and good specific surface area (S_{BET}= 625 m^2 g^{-1}). Under basic conditions, propranolol adsorption was favored for an adsorbent dosage of 0.7 g L^{-1}. The adsorbent showed fast kinetics, with the equilibrium influenced by the concentration. Avrami's model showed a satisfactory fit having a $t_{0.95}$ ranging from 47.8 to 179.3 min. Equilibrium data were best adjusted to the Liu isotherm model. The values of Q_{max} increased with the temperature, reaching up to 161.3 mg g^{-1} (45°C). The thermodynamic data showed $\Delta G° < 0$ for 298-328 K (adsorption process favorable) $\Delta H°$= + 7.403 kJ mol^{-1} (endothermic; magnitude compatible with physical adsorption), and $\Delta S°$= +115.2 J K^{-1} mol^{-1} (releases of water molecules of the adsorbate before it being adsorbed in the carbon surface). The biochar chemically activated with ZnCl2, produced from the leftover peels of Colombian palm fruits, is therefore inferred to be a promising option as an adsorbent for the treatment of effluents containing the medication propranolol hydrochloride.

Keywords: Adsorption; Residue; Activated biochar, adsorption thermodynamics, nonlinear Van't Hoff equation.

1. Introduction

Emerging micropollutants have attracted the scientific community's attention in recent years, as they are released in different sectors of society and can be detected in domestic, industrial, and, mainly, hospital effluents [1]. These residual compounds contaminate water resources and the soil, directly affecting the aquatic biota, the animals that consume this water, and even the plants. Therefore, in addition to techniques that remove these compounds, their long and medium-term effects must be studied [2,3]. Added to this, the United Nations (U.N.) has focused on sustainable development, which advocates the emergence of new environmental legislation policies on the global contamination of water resources, enabling studies on these ecological contaminants [1,4,5]. The class of drugs within emerging pollutants is a serious problem because while continuous discharges are released into the environment, they do not have environmental regulations [6–8]. It should be noted that even at low concentrations, these drugs may be quite hazardous to the aquatic biota, especially over an extended period [9–12].

The consumption of drugs used for hypertension has grown in recent years; propranolol hydrochloride ($C_{16}H_{21}NO_2$.HCl) is widely used worldwide, where the human body does not absorb a large part eliminated in the urine [13]. Propranolol (PROP) is highly persistent in the environment and has a long duration after consumption, with 4-hydroxypropranolol as its main metabolite [14,15]. Conventional processes used in the treatment of effluents partially remove this contaminant [13,16], the remainder being discharged into water bodies, highly harmful to various organisms such as the green algae *S. vacuolatus* [17]. In Brazil, PROP has been detected in surface, drinking, and effluents from water and sewage treatment plants [18,19]. Due to this problem, several techniques have been studied, mainly in removing and degrading this compound [1,20–23]. Adsorption has the advantage of applying new adsorbents from plant residues, mainly for producing carbon-based materials [24–27]. Normally, these carbonaceous materials, formed basically by carbon, have a good surface area and excellent pore development, some of the important characteristics of a good adsorbent [28,29].

The *Bactris guineensis* palm is an important fruit tree in the Colombian Caribbean extending to Central America. This fruit tree has great economic importance [30]. Popularly

known as corozo, its round and small fruits have a pulp with high nutritional value and can be consumed fresh and in the preparation of drinks, jellies, and even wines [31,32]. A single plant produces an average of 30 kg per year of fruit, reaching an annual productivity of 750 kg ha^{-1} [30], generating large volumes of residual biomass corresponding to bark and seeds. In addition, studies have reported that dark-colored pulp has an antioxidant action [31,33]. However, no studies reported residual biomass as a carbon precursor for preparing adsorbent material and possible application in removing emerging contaminants.

The activation process is one of the major steps to ensure that the adsorbent is able to remove or adsorb more molecules by creating pores and augmenting the textural proprieties [34]. Different activators can be used from salts, bases, and acids; among all the salts, the $ZnCl_2$ performs best, presenting a higher specific surface area and pore formation [35]. Therefore, enhancement of the textural proprieties is one of the most desired modifications that be done to the adsorption studies. In special, this modification technique tends to increase the adsorption capacity of the raw materials, allowing the molecules to diffuse more easily onto the pore and surface of the material [36].

Therefore, this use used the bark as the residual biomass of the *Bactris guineensis* fruit to prepare biochar chemically activated with zinc chloride ($ZnCl_2$) and subsequent use as an adsorbent. The main objective is to bring a new application for this residual biomass since it presents a large volume and high annual consumption in Latin countries such as Colombia. Another point is the problem of emerging contaminants such as propranolol, which has a small variety of adsorbents aimed at its removal. First, the pristine biomass and biochar material were characterized using different characterization techniques. Then activated biochar was used to remove the drug for hypertension propranolol hydrochloride. Next, adsorbent dosage and pH studies were carried out. Then kinetic and isothermal studies were determined, where the experimental data were fitted to specific mathematical models. Last, the thermodynamic parameters of adsorption were estimated.

2. Materials and methods

2.1 Chemical employed

The chemicals and reagents (further described) were all obtained from Sigma-Aldrich-USA in analytical grade. In order to adjust the pH, 0.1 M of HCl and NaOH were used. For activation in the carbonization step, zinc chloride salt ($ZnCl_2$) was used. The propranolol hydrochloride was used (chemical formula: $C_6H_{21}NO_2$.HCl; molecular weight: 295.807 g mol^{-1}) as adsorbate [1]. In order to obtain different concentrations of PROP, a stock solution was prepared. In this case, 1 g L^{-1} of PROP was dissolved in methanol due to the low solubility of the drug; in the end, a 1000 mg L^{-1} contraction solution was generated. Working solutions with different concentrations were attained by diluting the stock solution with deionized water and adjusting the solutions' pH using 0.1M NaOH or HCl (Digimed pHmeter, DM 20, Brazil).

2.2 Precursor gathering, pyrolysis, and characterization

The material gathered for pyrolysis and the characterization are specified in the Supplementary Material. In sum, the *Bactris guineenses* were obtained from a local producer in Barranquilla, Colombia. First, the fruit peel was separated, dried, and ground. After that, the powder was mixed with the activating agent ($ZnCl_2$) and pyrolyzed using a quartz reactor at N_2 atmosphere at 923.15 K. After that; the pyrolyzed material was washed with an HCl solution and dried. Finally, the source and pyrolyzed material were characterized through Fourier-transformed infrared spectroscopy, scanning electron microscopy, X-ray diffractometry, and N_2 adsorption and desorption isotherms (only for the pyrolyzed material).

2.3 Adsorption experiments with propanolol

All samples were continuously stirred at 150 rpm utilizing a thermostatic stirrer. The PROP concentration was determined through spectrophotometry using a UV micro 1240 (Shimadzu, Japan). The equipment was set to work at 255 nm, corresponding to the propanolol's maximum absorption wavelength. All assays were conducted in triplicates to guarantee the results' reliability; after each test, the samples were centrifuged at 5000 rpm for 15 min, separating the solid phase from the liquid phase; for details, see Supplementary material [37–42].

3. Results and Discussion

3.1. Characterization results of the source and pyrolyzed material

During the pyrolysis step, a good part of the lignin and cellulose is converted into volatile material, influencing the final yield and increasing the specific surface area [43]. Due to this process, the final carbonaceous skeleton formed basically by carbon presented a yield close to 29 %. This result agrees with other research using $ZnCl_2$ in proportions of 1:1. The biomasses used in this study were: jabuticaba residues [44], açai residues [45], fruits of the invasive species *Hovenia dulcis* [46] and cassava peels [47]. When using KOH as an activating agent, the authors reported a yield close to 64% [48]. The biochar developed from *Bactris guineensis* residues obtained a satisfactory surface area of 625 $m^2\ g^{-1}$ (Figure 1a). Figure 1b allows classifying the isotherms as type I (IUPAC); these structures correspond to micro and mesoporous materials [49,50]. The H4-type hysteresis slit is typical of structures with pores with diameters equal to those obtained in this study [50]. The results corroborate the developed carbonaceous material's pore volume (0.4223 $cm^3\ g^{-1}$). Analyzing the textural properties of the adsorbent is essential because they strongly influence the adsorption performance [51]. When observing structures composed of lignin and cellulose and carbonized with $ZnCl_2$, we observed similar characteristics to this study [52–54].

<Fig.1>

Figure 2 makes it possible to identify the main functional groups present on the surface of the materials. It is possible to observe that most groups remained after carbonization with a lower intensity. The bad at 3441 cm^{-1} (biochar) and 3445 cm^{-1} (biomass), the O-H bonding occurs [55]. The bands at 2922 and 2854 cm^{-1} (BC) and 2923 and 2855 cm^{-1} (biomass) are assigned to asymmetric and symmetric C-H stretch bonds, respectively [56]. The band at the 1738 cm^{-1} region is assigned to C=O bonds in ketones, and aldehydes are found in the biomass precursor [58]. However, in biochar, the disappearance of the C=O bond corroborates the loss of volatile material during pyrolysis [57].

The carboxylate stretching vibrations correspond to the band at 1631 cm^{-1} (biochar) and 1641 (biomass) [59]. The band at 1451 cm^{-1} in the biomass can be assigned to the C-H bending of lignocellulosic material or ring modes of aromatics in lignin [57,60]; this band

157 vanished in the biochar material. On the other hand, the bands at 1379 cm^{-1} (carbon
158 precursor) and 1383 cm^{-1} (biochar) can be assigned to C-H bending [57,60]. The band at 1254
159 cm^{-1} (carbon precursor) is assigned to the C-O stretching of phenol present in lignin [29, 61].
160 The bands at 1107 cm^{-1} (carbon precursor) and 1153 and 1114 cm^{-1} (biochar) are assigned to
161 attributed to C-O-C of ether and C-C-O of esther stretching [29], and the peak at 1043 cm^{-1}
162 (carbon precursor) is attributed to C-O stretching of phenolic groups or carboxylate [29; 61].
163]. The band at 897 cm^{-1} (carbon precursor) and 801 cm^{-1} (biochar) are attributed to the C-H
164 bending of aromatics [29]. The FTIR results of this work are similar to those obtained by
165 Bouchelta et al. [58] by carbonizing date fruit waste.

166 <Fig.2>

167 Figure 3 corresponds to the XRD patterns of the source and pyrolyzed samples.
168 Firstly, the long diffraction band between 15 and 30 corresponds to the presence of
169 amorphous carbon [62]. This band undergoes changes after carbonization, where its width
170 decreases and its intensity increases, which may be related to a more organized structure
171 formed after the pyrolysis; however, the biochar material is still amorphous. Amorphous
172 arrangements are usually disorganized and irregular. However, they have empty spaces in
173 their organization, which can be occupied by adsorbate molecules, supporting the adsorption
174 [24].

175 <Fig.3>

176 The high temperature employed together with the activation provided apparent
177 morphological modifications to the surface of the materials (Fig. 4). Initially, the irregular
178 particles of different sizes had a uniform and smooth surface (Fig. 4a). However, when they
179 were carbonized, they started to contain numerous irregularities and protuberances (Fig. 4b).
180 Materials formed by lignin and cellulose tend to have irregular and disorganized
181 morphological structures, such as tree bark [63–66], fruit residues [44,67–70] and seeds of
182 forest species [71–74]. These irregularities are alternately distributed and present cavities and
183 empty spaces, which can be highly favorable for adsorption [46,70].

184 <Fig.4>

185 *3.2. Study of adsorbent dosage and pH*

The optimal BC dosage (Figure 5) was determined using 25 mg L^{-1} of PROP. In the process of increased dosage from 0.5 to 1 g L^{-1}, the capacity decreases from 75 to 51 mg g^{-1}, while the removal shows the opposite behavior, increasing from 70 to 96%. The curves are crossed at 0.7 g L^{-1} dosage, presenting a q value of 64 mg g^{-1} and a removal percentage of 64 %, which is fairly good. Therefore, 0.7 g L^{-1} of BC was utilized for the next adsorption experiments. When using ionic liquid iron nanocomposite as an adsorbent in the removal of PROP, it was observed that increasing the dosage from 0.05 to 0.5 g L^{-1} generated an increase in removal from 30 to 90 % [75].

<Fig.5>

The effect of the pH of the solution was analyzed according to Figure 6. Initially, when the adsorbate solution pH is acidic (pH 3), the adsorption capacity is 30.6 mg g^{-1}; when raising the pH to 6, the capacity drops to 26.8 mg g^{-1}. From pH 6, the capacity increases until reaching the capacity of 33.56 mg g^{-1} at pH 8. Then the capacity suffers a slight decrease up to pH 10. This behavior confirms that the incremental change of the solution pH, close to 8, favors the adsorption of the PROP. This result corroborates the study by Ali et al. [75], whereby by raising the pH from 3 to 11, the adsorption capacity of PROP rises to a pH close to 9 and then decreases again. PROP presents constant acidity being a secondary amine (pK_a=9.5). Therefore, the charges of the β-blockers present in the solution are mostly positive, favoring adsorption at high pH. At pH > 8, the amine is released by hydrolysis and precipitated due to its low solubility, making adsorption above this value unfeasible [76]. Added to this, the point of zero charge of the adsorbent was 6.5, so when the pH is at this value, the charges on the surface are equal to zero. When the pH value is above 6.5, the surface is negatively charged; when the pH is below 6.5, the surface of the adsorbent is positively charged. Therefore, electrostatic repulsion occurs under acidic conditions, and electrostatic attraction occurs under basic conditions. In this study, pH 8 was fixed for further experiments.

<Fig.6>

3.3. Propranolol adsorption kinetics

By means of three concentrations, the performance of the carbonaceous material in the PROP uptake and the time to attain the equilibrium were analyzed according to the kinetic curves represented in Figure 7.

The experimental kinetic data were adjusted to the Pseudo-first-order (PFO), Pseudo-second-order (PSO), and Avrami fractional-order (AFO) models (see Table S1). The AFO presented the bested values of R^2_{adj}, followed by the PSO and PFO. This same tendency was obtained for the statistical parameter SD (mg g^{-1}), with the lowest values reached by the AFO, followed by the PSO and PFO [77–80]. Also, to confirm the best kinetic model, the BIC analysis was carried out. The values of BIC for AFO were always lower than PFO and PSO. Therefore, the ΔBIC of the two models can be conclusive for $\Delta BIC < 2$ (the two models have no significant differences) or $\Delta BIC \geq 10$ (indicates that the model with the lowest BIC is surely the best-fitted) [37,38]. On the other hand, for $2 < \Delta BIC < 6$, the model with a lower BIC value has a possibility of being the best-fitted model, or $6 < \Delta BIC < 10$, the model with a lower BIC value has a strong possibility of being the best-fitted model [37,38]. The ΔBIC for PFO and Avrami were always higher than 10; therefore, PFO does not explain the kinetic results properly [37,38]. The ΔBIC between PSO and Avrami was higher than 10 for C_o PROP of 50 and 75 mg/L, being AFO the best kinetic model [37,38]. However, for C_o 25 mg L^{-1} PROP, the ΔBIC between PSO and AFO was 7.063, with a high likelihood that the optimum kinetic model is the AFO. Therefore, AFO satisfactorily explains the kinetic data considering the set of the three concentrations of PROP [37,38].

Another important piece of information shown in Table S1 is the values of $t_{1/2}$ and $t_{0.95}$ [38], which are defined as the time necessary to attain 50% and 95% of the maximum sorption capacity described by the model curve. Considering that AFO was the best-fitted kinetic model, it was observed that $t_{1/2}$ for the uptake of PROP onto the BC ranged from 4.354 min (C_o 25 mg/L) to 15.02 min (C_o 75 mg/L), and $t_{0.95}$ for the uptake of PROP onto BC ranged from 47.82 (C_o 25 mg/L) to 179.3 min (C_o 75 mg/L). These results show that increased sorption capacity leads to increased time to attain equilibrium. Considering that the isotherms were performed with C_o up to 150 mg/L of PROP, thus, it is advisable to employ a contact time of at least 240 min to perform the adsorption equilibrium experiments. Therefore, it is possible to conclude that the batch system may operate for around 15 min at a higher concentration before the need for regeneration.

When analyzing the kinetic behavior of PROP by other adsorbents in the literature, we observed that there are fast and slow kinetics cases. For example, when analyzing the adsorption of PROP on montmorillonite clay, the authors observed that about 96% of the drug

had already been removed in the first minute, confirming the high affinity of the adsorbent with the adsorbate [76]. Conversely, using Na-mica-4 and C18-mica-4, the authors took 24 hours to achieve 97 % removal in river water samples synthetically contaminated with PROP [81]. Finally, when using granular activated carbon, the authors reported 88% and 68 % removal in 90 min [82] and 180 min [83], respectively.

<Fig.7>

3.4. Isothermal studies and estimation of thermodynamic parameters of adsorption

Isothermal studies were carried out at temperatures of 298, 308, 318, and 328 K, which resulted in the construction of four equilibrium curves (Fig. 8). These data help elucidate the interaction between BC and PROP and allow to calculate the parameters of thermodynamics of adsorption ($\Delta G°$, $\Delta H°$, and $\Delta S°$). The curves were constructed by varying the concentration from 25 to 150 mg L^{-1} of PROP. As a result, all curves show identical and favorable behavior for L-shaped adsorption [84].

<Fig.8>

The experimental equilibrium data fit the Langmuir, Freundlich, and Liu models (see Table S2). When analyzing the adjusted determination coefficients (R^2_{adj}), it was verified that their values were closer to 1 using the Langmuir isotherm at the temperature of 298K. Liu for the temperature of 308 to 328 K. This statistical parameter was followed by SD, whose lowest values were obtained by the Langmuir model at 298 K, and Liu from 308 to 328 K. It was evident that the Freundlich isotherm model had the lowest values of R^2_{adj} and higher values of SD for all the temperatures, indicating that Freundlich isotherm model is not adequate to model the equilibrium data. Therefore, the BIC was utilized to verify what is the best isotherm model because it can be conclusive when $\Delta BIC < 2$ (the difference between the two models is not statistically significant) or $\Delta BIC \geq 10$ (indicates that the model with the lowest BIC is surely the best-fitted) [37,38]. At 298 K, the ΔBIC between the Langmuir and Liu models was 1.606, indicating no relevant differences between the two isotherm models; both models can represent the equilibrium at 298 K. On the other hand, for 308, 318, and 328K, the ΔBIC between Liu and Langmuir were 70.70, 73.35, and 82.99, respectively, inferring that

undoubtedly, the Liu isotherm model is the best-fitted equilibrium model for representing the equilibrium data from 308 to 328 K. Considering that at 298 K, the differences of Liu and Langmuir were not significatively different, it could be stated that for the 298-328 K, the Liu model is the best equilibrium model to represent the experimental equilibrium data.

Also, it was observed that for both Langmuir and Liu isotherm models, the values of Q_{max} increased with the temperature. Considering that the Liu isotherm model best described the equilibrium data, it could be stated that the Q_{max} varied from 124.5 at 298 K to 161.3 mg g^{-1} at 328 K. The increasing maximum sorption uptake with the temperature is due to the driving force gradient that increases with the adsorbate concentration [85]. To be more precise, the temperature increase can affect the mass transport mechanism by changing the external and internal mass transfer mechanism [36]. The external mass transfer depends on the film formed between the adsorbent and the aqueous phase, named the boundary layer. This layer can be affected by external forces such as velocity and temperature; thus, increasing the temperature diminishes the mass transfer resistance [86]. As the internal mass transfer is based on pore and surface diffusion, these phenomena are also a function of the textural proprieties and the experimental conditions. The temperature increase tends to increase pore diffusion, according to Willke-Chang [87], which also affects surface diffusion. Although studies analyzing the adsorption of PROP are few compared to other emerging pollutants, some studies confirm results similar to those obtained in this study. For example, when analyzing the adsorption of PROP in bentonite clay, the authors observed that the capacities increased from 0.298 to 0.426 mmol g^{-1} with the increase in temperature from 293 to 313 K [1].

When analyzing the maximum capacity obtained by the model (161.3 mg g^{-1}) and comparing it with other reports, it is concluded that the residual peels of the carbonized *Bactris guineensis* fruits have a high potential for application concerning effluents containing PROP. When bentonite clay was employed as an adsorbent, a capacity of 0.468 mmol g^{-1} for the concentration of 0.05 to 3 mmol L^{-1} of PROP was observed [1]. The maximum capacity of 6.2 x 105 µmol g^{-1} was obtained using Montmorillonite as an adsorbent, varying the concentration from 0.5 to 80 mg L^{-1} [76]. With nanocomposite, the capacity was 105.26 µg g^{-1} for a concentration of 10-70 µg mL^{-1} [75]. Using corn husk biochar, the authors reported a capacity of 6.67 µmol m^{-2} for a concentration of 0.800-30 mg L^{-1} [88]. Finally, a Q_{max} of 287 mg

306 g^{-1} was reported using p-doped mesoporous carbon with a concentration of 100 mg L^{-1} [89].
307 A study on a fixed bed system with magnetic tire char reported a capacity of 22.58 mg g^{-1} [90].
308 This means that the developed adsorbent can compete on par with other adsorbents in
309 removing PROP and providing an application for the residue.
310

311 The thermodynamic parameters were obtained based on the equilibrium constants
312 obtained from the equilibrium isotherms using the nonlinear Van't Hoff equation (Table S3)
313 [37–42].

314 The K_e^0 was obtained through the best-fit isotherm fitted in the 298-328 K interval (Liu)
315 [37–42]. The thermodynamic parameters were obtained as described in the Supplementary
316 Material [37–42]. The K_e^0 values augmented from $5.234.10^4$ to $6.886.10^4$ as the temperature
317 increased from 298 to 328 K, confirming that the adsorption process is endothermic.
318 Conversely, ΔG^0 decreased from -26.92 (298 K) to -30.38 kJ mol^{-1} (328 K), indicating that the
319 adsorption of PROP in the carbonaceous adsorbent was favorable and spontaneous. However,
320 ΔH^0 is positive (7.403 kJ mol^1), indicating an endothermic process. The magnitude of ΔH^0 is
321 compatible with the physical interactions of the PROP with BC. These interactions may be van
322 der Waals forces, π-π interactions [38]. Based on this study, the adsorption process is physical
323 adsorption. Furthermore, ΔS^0 +115.2 J mol^{-1} K^{-1} suggests that the PROP was hydrated before
324 being uptaken by the adsorbent, and releasing hydration waters increased the entropy when
325 PROP molecules were adsorbed. In the literature, the study of the propranolol uptake from
326 aqueous solutions in thermally treated bentonite clay also confirmed the behavior of an
327 endothermic nature [1].
328

329 *3.5. Proposed reaction mechanism*

330 One can suggest an adsorption mechanism by taking into account the outcomes of the
331 adsorbent's characterization, speciation, and standard enthalpy change's magnitude. First, the
332 FT-IR results should be considered to propose a bare minimum adsorption surface. In this case,
333 classical groups for activated biochar were found: C-H, C=O, OH (phenolic), and aromatic rings.
334 Considering that the point of zero charge of the adsorption is 6.4, thus for solution pH > 6.4,
335 the adsorbent surface will be negatively charged (see Fig S.1). Another important factor is the

speciation of the adsorbate, in this case, the PROP, has two states one neutral and other protonated, due to the amine group (see Fig S.2). Last, the thermodynamic magnitude $\Delta H°$, indicates the nature of the bond, in this case being classified as physical interaction. Taking into consideration all the aspects of the system is possible to propose the mechanism, according to Figure 9. The PROP is expected to be adsorbed on the surface due to hydrogen bonds, Van de Waals interaction, or ion-π interaction.

<Fig.9>

4. Conclusion

Residual peels of the edible fruit *Bactris guineensis*, native to the Colombian Caribbean, were successfully charred with zinc chloride. For the literature, this study provides a new use for this residue, where carbonization with zinc chloride makes it possible to obtain an adsorbent with good textural characteristics and with great potential for adsorption in solutions contaminated with PROP. The adsorbent showed good superficial characteristics (S_{BET}=625 m^2 g^{-1}; V_T= 4.223x10^{-1} cm^3 g^{-1}). The dosage of 0.7 g L^{-1} and the pH of 8 favored the adsorption of the drug on the activated charcoal surface. The system equilibrium was influenced by the concentration, being faster at the lowest concentration (25 mg L^{-1}) and longer at the highest concentration (75 mg L^{-1}). According to $t_{0.95}$ obtained from the Avrami-fractional model, the time to attain 95% saturation ranged from 47.82 (25 mg L^{-1}) to 179.3 min (75 mg L^{-1}). Avrami's model represented the kinetic data well. The increase in temperature in the system confirmed a favoring of the adsorbate with the adsorbent. With the maximum capacity obtained (161.3 mg g^{-1}) at 328 K based on the Liu isotherm model. The thermodynamic parameters confirmed a physical and endothermic process (ΔH^0 = 7.403 kJ mol^{-1}).

Therefore, applying the residual biomass generated by the *Bactris guineensis* palm fruit production chain as biomass for producing activated biochar has great potential. Its use as an adsorbent in solutions containing propranolol hydrochloride can be used successfully and efficiently. Future perspectives are to develop new coals with this biomass, applying possible new activating agents. Analyzing the adsorption capacity of these new biochars with other emerging pollutants is also possible. A pilot study in a fixed bed column is highly necessary for

possible large-scale applications. Therefore, the analysis of the adsorbent through continuous systems must also be studied. With this, parameters such as the amount of adsorbent mass, flow rates, and concentrations must be analyzed. After analyzing and defining the studies in continuous systems, it is necessary to overcome the barrier between the scientific society and society, in this case, the industries. At first, when the skin is left over from consumption along with other remains of the same species, it would be interesting to create collection points in large markets in the largest cities. In addition, the entire industrial process that generates the waste must be willing to supply this waste. Thus, the residues from two sources should be sent to a processing industry, where rotary kilns with the activating agent are used to generate activated carbon. Finally, it is necessary to create charcoal pellets to ensure material resistance and possible application in other industrial processes and water treatment.

Acknowledgment

E.C. Lima thanks to CNPq (Conselho Nacional de Desenvolvimento Científico e Tecnológico) for the projects 303.612/2021-5 and 402.450/2021-3 and FINEP (Financiadora de Estudos e Projetos) for the Project 044/21/IAP 1942/FAURGS 8638 for financial support and fellowships.

5. References

[1] D. Cristina do Nascimento, M. Gurgel Carlos da Silva, M. Gurgel Adeodato Vieira, Adsorption of propranolol hydrochloride from aqueous solutions onto thermally treated bentonite clay: A complete batch system evaluation, J. Mol. Liq. 337 (2021). https://doi.org/10.1016/j.molliq.2021.116442.

[2] J.C.V. Sposito, C.C. Montagner, M. Casado, L. Navarro-Martín, J.C. Jut Solórzano, B. Piña, A.B. Grisolia, Emerging contaminants in Brazilian rivers: Occurrence and effects on gene expression in zebrafish (Danio rerio) embryos, Chemosphere. 209 (2018) 696–704. https://doi.org/10.1016/J.CHEMOSPHERE.2018.06.046.

[3] C.C. Montagner, F.F. Sodré, R.D. Acayaba, C. Vidal, I. Campestrini, M.A. Locatelli, I.C. Pescara, A.F. Albuquerque, G.A. Umbuzeiro, W.F. Jardim, Ten years-snapshot of the occurrence of emerging contaminants in drinking, surface and ground waters and wastewaters from São Paulo State, Brazil, J. Braz. Chem. Soc. 30 (2019) 614–632. https://doi.org/10.21577/0103-5053.20180232.

[4] J. Georgin, D.S.P. Franco, K. Da Boit Martinello, E.C. Lima, L.F.O. Silva, A review of the toxicology presence and removal of ketoprofen through adsorption technology, J. Environ. Chem. Eng. 10 (2022) 107798. https://doi.org/10.1016/j.jece.2022.107798.

[5] R. Ozola-Davidane, J. Burlakovs, T. Tamm, S. Zeltkalne, A.E. Krauklis, M. Klavins, Bentonite-ionic liquid composites for Congo red removal from aqueous solutions, J. Mol. Liq. 337 (2021) 116373. https://doi.org/10.1016/j.molliq.2021.116373.

[6] B. Petrie, R. Barden, B. Kasprzyk-Hordern, A review on emerging contaminants in wastewaters and the environment: Current knowledge, understudied areas and recommendations for future monitoring, Water Res. 72 (2015) 3–27. https://doi.org/10.1016/j.watres.2014.08.053.

[7] N.H. Tran, M. Reinhard, K.Y.H. Gin, Occurrence and the fate of emerging contaminants in municipal wastewater treatment plants from different geographical regions-a review, Water Res. 133 (2018) 182–207. https://doi.org/10.1016/j.watres.2017.12.029.

[8] L. Sbardella, J. Comas, A. Fenu, I. Rodriguez-Roda, M. Weemaes, Advanced biological activated carbon filter for removing pharmaceutically active compounds from treated wastewater, Sci. Total Environ. 636 (2018) 519–529. https://doi.org/10.1016/j.scitotenv.2018.04.214.

[9] J.R. De Andrade, M.F. Oliveira, M.G.C. Da Silva, M.G.A. Vieira, Adsorption of Pharmaceuticals from Water and Wastewater Using Nonconventional Low-Cost Materials: A Review, Ind. Eng. Chem. Res. 57 (2018) 3103–3127. https://doi.org/10.1021/acs.iecr.7b05137.

[10] J. Menz, A.P. Toolaram, T. Rastogi, C. Leder, O. Olsson, K. Kümmerer, M. Schneider, Transformation products in the water cycle and the unsolved problem of their proactive assessment: A combined in vitro/in silico approach, Environ. Int. 98 (2017) 171–180. https://doi.org/10.1016/j.envint.2016.11.003.

[11] W.T. Vieira, M.B. de Farias, M.P. Spaolonzi, M.G.C. da Silva, M.G.A. Vieira, Removal of endocrine disruptors in waters by adsorption, membrane filtration, and biodegradation. A review, Springer International Publishing, 2020. https://doi.org/10.1007/s10311-020-01000-1.

[12] V. Arya, L. Philip, Adsorption of pharmaceuticals in water using Fe3O4 coated polymer clay composite, Microporous Mesoporous Mater. 232 (2016) 273–280. https://doi.org/10.1016/j.micromeso.2016.06.033.

[13] D. Ashton, M. Hilton, K. V. Thomas, Investigating the environmental transport of human pharmaceuticals to streams in the United Kingdom, Sci. Total Environ. 333 (2004) 167–184. https://doi.org/10.1016/j.scitotenv.2004.04.062.

[14] T. Rastogi, C. Leder, K. Kümmerer, Re-Designing of Existing Pharmaceuticals for Environmental Biodegradability: A Tiered Approach with β-Blocker Propranolol as an Example, Environ. Sci. Technol. 49 (2015) 11756–11763. https://doi.org/10.1021/acs.est.5b03051.

[15] C.G. Daughton, T.A. Ternes, Pharmaceuticals and personal care products in the environment: Agents of subtle change?, Environ. Health Perspect. 107 (1999) 907–938. https://doi.org/10.1289/ehp.99107s6907.

[16] G. Sim, E.C. Lima, S.H. Larsson, F.G. Gentili, Microalgae biomass as a sustainable precursor to produce nitrogen-doped biochar for efficient removal of emerging

pollutants from aqueous media, 348 (2022). https://doi.org/10.1016/j.jclepro.2022.131280.

[17] J. Maszkowska, S. Stolte, J. Kumirska, P. Łukaszewicz, K. Mioduszewska, A. Puckowski, M. Caban, M. Wagil, P. Stepnowski, A. Białk-Bielińska, Beta-blockers in the environment: Part II. Ecotoxicity study, Sci. Total Environ. 493 (2014) 1122–1126. https://doi.org/10.1016/j.scitotenv.2014.06.039.

[18] C. Peña-Guzmán, S. Ulloa-Sánchez, K. Mora, R. Helena-Bustos, E. Lopez-Barrera, J. Alvarez, M. Rodriguez-Pinzón, Emerging pollutants in the urban water cycle in Latin America: A review of the current literature, J. Environ. Manage. 237 (2019) 408–423. https://doi.org/10.1016/j.jenvman.2019.02.100.

[19] M.C.V.M. Starling, C.C. Amorim, M.M.D. Leão, Occurrence, control, and the fate of contaminants of emerging concern in environmental compartments in Brazil, J. Hazard. Mater. (2019) 17–36. https://doi.org/10.1016/j.jhazmat.2018.04.043.

[20] H.T.B. Phan, A.Q.K. Nguyen, Y.Y. Ahn, K. Kim, S. Kim, J. Kim, Visible light-induced degradation of propranolol with peroxymonosulfate as an oxidant and a radical precursor, Sep. Purif. Technol. 289 (2022) 120764. https://doi.org/10.1016/j.seppur.2022.120764.

[21] G.L. Colpani, V.F. Santos, R.C.F. Zeferino, M. Zanetti, J.M.M. de Mello, L.L. Silva, N. Padoin, R. de F.P.M. Moreira, M.A. Fiori, C. Soares, Propranolol hydrochloride degradation using La@TiO2 functionalized with CMCD, J. Rare Earths. 40 (2022) 579–585. https://doi.org/10.1016/j.jre.2021.03.002.

[22] Y. Ding, K. Cui, X. Liu, Q. Xie, Z. Guo, Y. Chen, Lignin peroxidase-catalyzed direct oxidation of trace organic pollutants through a long-range electron transfer mechanism: Using propranolol as an example, J. Hazard. Mater. 431 (2022) 128544. https://doi.org/10.1016/j.jhazmat.2022.128544.

[23] A.B. Rakhym, G.A. Seilkhanova, Y. Mastai, Physicochemical evaluation of the effect of natural zeolite modification with didodecyl-dimethyl-ammonium bromide on the adsorption of Bisphenol-A and Propranolol Hydrochloride, Microporous Mesoporous Mater. 318 (2021) 111020. https://doi.org/10.1016/j.micromeso.2021.111020.

[24] D.S.P. Franco, J. Georgin, E.C. Lima, L.F.O. Silva, Journal of Water Process Engineering Advances made in removing paraquat herbicide by adsorption technology : A review, J. Water Process Eng. 49 (2022) 102988. https://doi.org/10.1016/j.jwpe.2022.102988.

[25] A. Bhatnagar, M. Sillanpää, Utilization of agro-industrial and municipal waste materials as potential adsorbents for water treatment-A review, Chem. Eng. J. 157 (2010) 277–296. https://doi.org/10.1016/j.cej.2010.01.007.

[26] M. Guy, M. Mathieu, I.P. Anastopoulos, G. Mart, G.L. Dotto, H.P. De Oliveira, E.C. Lima, M. Thyrel, S.H. Larsson, G.S. Reis, Graphitic Biochars for Efficient Azo Dye Adsorption, (2022).

[27] S. Glaydson, M. Guy, M. Mathieu, M. Jebrane, E.C. Lima, M. Thyrel, G.L. Dotto, S.H. Larsson, Colloids and Surfaces A : Physicochemical and Engineering Aspects A comparative study of chemical treatment by $MgCl_2$, $ZnSO_4$, $ZnCl_2$, and KOH on

physicochemical properties and acetaminophen adsorption performance of biobased porous materials from tree bark residues, Colloids Surfaces A Physicochem. Eng. Asp. 642 (2022) 128626. https://doi.org/10.1016/j.colsurfa.2022.128626.

[28] A.H. Jawad, A. Saud Abdulhameed, L.D. Wilson, S.S.A. Syed-Hassan, Z.A. ALOthman, M. Rizwan Khan, High surface area and mesoporous activated carbon from KOH-activated dragon fruit peels for methylene blue dye adsorption: Optimization and mechanism study, Chinese J. Chem. Eng. 32 (2021) 281–290. https://doi.org/10.1016/j.cjche.2020.09.070.

[29] N.F.G.M. Cimirro, E.C. Lima, M.R. Cunha, P.S. Thue, A. Grimm, G.S. dos Reis, N. Rabiee, M.R. Saeb, F. Keivanimehr, S. Habibzadeh, Removal of diphenols using pine biochar. Kinetics, equilibrium, thermodynamics, and mechanism of uptake, J. Mol. Liq. 364 (2022) 119979. https://doi.org/10.1016/j.molliq.2022.119979.

[30] E. Brieva-Oviedo, A.C.D. Maia, L.A. Núñez-Avellaneda, Pollination of Bactris guineensis (Arecaceae), a potential economically exploitable fruit palm from the Colombian Caribbean, Flora Morphol. Distrib. Funct. Ecol. Plants. 269 (2020) 151628. https://doi.org/10.1016/j.flora.2020.151628.

[31] C. Osorio, J.G. Carriazo, O. Almanza, Antioxidant activity of corozo (Bactris guineensis) fruit by electron paramagnetic resonance (EPR) spectroscopy, Eur. Food Res. Technol. 233 (2011) 103–108. https://doi.org/10.1007/s00217-011-1499-4.

[32] C. Diaz-Uribe, W. Vallejo, E. Romero, M. Villareal, M. Padilla, N. Hazbun, A. Muñoz-Acevedo, E. Schott, X. Zarate, TiO2 thin films sensitization with natural dyes extracted from Bactris guineensis for photocatalytic applications: Experimental and DFT study, J. Saudi Chem. Soc. 24 (2020) 407–416. https://doi.org/10.1016/j.jscs.2020.03.004.

[33] L.G. Sequeda-Castañeda, A.R. Barrera-Bugallo, C. Celis, J. Iglesias, L. Morales, Evaluation of the antioxidant and cytotoxic activity of extracts from fruits in fibroblastoma HT1080 cell lines: Four fruits with commercial potential in Colombia, Emirates J. Food Agric. 28 (2016) 143–151. https://doi.org/10.9755/ejfa.2015-11-1007.

[34] J. Bedia, M. Peñas-Garzón, A. Gómez-Avilés, J.J. Rodriguez, C. Belver, Review on Activated Carbons by Chemical Activation with FeCl3, C — J. Carbon Res. 6 (2020) 21. https://doi.org/10.3390/c6020021.

[35] Y. Gao, Q. Yue, B. Gao, A. Li, Insight into activated carbon from different kinds of chemical activating agents: A review, Sci. Total Environ. 746 (2020) 141094. https://doi.org/10.1016/j.scitotenv.2020.141094.

[36] R. Leyva-Ramos, C.J. Geankoplis, Model simulation and analysis of surface diffusion of liquids in porous solids, Chem. Eng. Sci. 40 (1985) 799–807. https://doi.org/10.1016/0009-2509(85)85032-6.

[37] E.C. Lima, F. Sher, A. Guleria, M.R. Saeb, I. Anastopoulos, H.N. Tran, A. Hosseini-Bandegharaei, Is one performing the treatment data of adsorption kinetics correctly?, J. Environ. Chem. Eng. 9 (2021) 104813. https://doi.org/10.1016/j.jece.2020.104813.

[38] É.C. Lima, M.H. Dehghani, A. Guleria, F. Sher, R.R. Karri, G.L. Dotto, H.N. Tran, Adsorption: Fundamental aspects and applications of adsorption for effluent

treatment, in: M. Hadi Dehghani, R. Karri, E. Lima (Eds.), Green Technol. Defluoridation Water, Elsevier, 2021: pp. 41–88. https://doi.org/10.1016/b978-0-323-85768-0.00004-x.

[39] E.C. Lima, A. Hosseini-Bandegharaei, I. Anastopoulos, Response to "Some remarks on a critical review of the estimation of the thermodynamic parameters on adsorption equilibria. Wrong use of equilibrium constant in the van't Hoff equation for calculation of thermodynamic parameters of adsorption - Journal of, J. Mol. Liq. 280 (2019) 298–300. https://doi.org/10.1016/j.molliq.2019.01.160.

[40] E.C. Lima, A. Hosseini-Bandegharaei, I. Anastopoulos, J.C. Moreno-Piraján, I. Anastopoulos, A critical review of the estimation of the thermodynamic parameters on adsorption equilibria. Wrong use of equilibrium constant in the Van't Hoof equation for calculation of thermodynamic parameters of adsorption, J. Mol. Liq. 273 (2019) 425–434. https://doi.org/10.1016/j.molliq.2018.10.048.

[41] E.C. Lima, A.A. Gomes, H.N. Tran, Comparison of the nonlinear and linear forms of the van't Hoff equation for calculation of adsorption thermodynamic parameters (ΔS° and ΔH°), J. Mol. Liq. 311 (2020) 113315. https://doi.org/10.1016/j.molliq.2020.113315.

[42] H.N. Tran, E.C. Lima, R.-S. Juang, J.-C. Bollinger, H.-P. Chao, Thermodynamic parameters of liquid–phase adsorption process calculated from different equilibrium constants related to adsorption isotherms: A comparison study, J. Environ. Chem. Eng. 9 (2021) 106674. https://doi.org/10.1016/j.jece.2021.106674.

[43] O. Üner, Y. Bayrak, The effect of carbonization temperature, carbonization time and impregnation ratio on the properties of activated carbon produced from Arundo donax, Microporous Mesoporous Mater. 268 (2018) 225–234. https://doi.org/10.1016/j.micromeso.2018.04.037.

[44] D.S.P. Franco, J. Georgin, M.S. Netto, K. da Boit Martinello, L.F.O. Silva, Preparation of activated carbons from fruit residues for the removal of naproxen (NPX): Analytical interpretation via statistical physical model, J. Mol. Liq. 356 (2022) 119021. https://doi.org/10.1016/j.molliq.2022.119021.

[45] R. Ramirez, C.E. Schnorr, J. Georgin, M.S. Netto, D.S.P. Franco, E. Carissimi, D. Wolff, L.F.O. Silva, G.L. Dotto, Transformation of Residual Açai Fruit (Euterpe oleracea) Seeds into Porous Adsorbent for Efficient Removal of 2,4-Dichlorophenoxyacetic Acid Herbicide from Waters, Molecules. 27 (2022) 7781. https://doi.org/10.3390/molecules27227781.

[46] J. Georgin, D.S.P. Franco, M.S. Netto, B.M.V. Gama, D.P. Fernandes, P. Sepúlveda, L.F.O. Silva, L. Meili, Effective adsorption of harmful herbicide diuron onto novel activated carbon from Hovenia dulcis, Colloids Surfaces A Physicochem. Eng. Asp. 654 (2022) 129900. https://doi.org/10.1016/j.colsurfa.2022.129900.

[47] J. Georgin, D. Pinto, D.S.P. Franco, M.S. Netto, J.S. Lazarotto, D.G. Allasia, R. Tassi, L.F.O. Silva, G.L. Dotto, Improved Adsorption of the Toxic Herbicide Diuron Using Activated Carbon Obtained from Residual Cassava Biomass, (2022).

[48] V.E. Efeovbokhan, E.E. Alagbe, B. Odika, R. Babalola, T.E. Oladimeji, O.G. Abatan, E.O. Yusuf, Preparation and characterization of activated carbon from plantain peel and

564 coconut shell using biological activators, J. Phys. Conf. Ser. 1378 (2019).
565 https://doi.org/10.1088/1742-6596/1378/3/032035.

566 [49] K.S.W. Sing, Reporting physisorption data for gas / solid systems with Special Reference
567 to the Determination of S, Pure Appl. Chem. 54 (1982) 2201–2218.
568 https://doi.org/10.1515/iupac.57.0007.

569 [50] M. Thommes, K. Kaneko, A. V. Neimark, J.P. Olivier, F. Rodriguez-Reinoso, J. Rouquerol,
570 K.S.W. Sing, Physisorption of gases, with special reference to the evaluation of the
571 surface area and pore size distribution (IUPAC Technical Report), Pure Appl. Chem. 87
572 (2015) 1051–1069. https://doi.org/10.1515/pac-2014-1117.

573 [51] E.M. Cuerda-Correa, J.R. Domínguez-Vargas, F.J. Olivares-Marín, J.B. de Heredia, On the
574 use of carbon blacks as potential low-cost adsorbents for the removal of non-steroidal
575 anti-inflammatory drugs from river water, J. Hazard. Mater. 177 (2010) 1046–1053.
576 https://doi.org/10.1016/j.jhazmat.2010.01.026.

577 [52] M. Guo, J. Wang, C. Wang, P.J. Strong, P. Jiang, Y.S. Ok, H. Wang, Carbon nanotube-
578 grafted chitosan and its adsorption capacity for phenol in aqueous solution, Sci. Total
579 Environ. 682 (2019) 340–347. https://doi.org/10.1016/j.scitotenv.2019.05.148.

580 [53] M. Bounaas, A. Bouguettoucha, D. Chebli, J.M. Gatica, H. Vidal, Role of the Wild Carob
581 as Biosorbent and as Precursor of a New High-Surface-Area Activated Carbon for the
582 Adsorption of Methylene Blue, Arab. J. Sci. Eng. 46 (2021) 325–341.
583 https://doi.org/10.1007/s13369-020-04739-5.

584 [54] A. Yazidi, M. Atrous, F. Edi Soetaredjo, L. Sellaoui, S. Ismadji, A. Erto, A. Bonilla-
585 Petriciolet, G. Luiz Dotto, A. Ben Lamine, Adsorption of amoxicillin and tetracycline on
586 activated carbon prepared from durian shell in single and binary systems: Experimental
587 study and modeling analysis, Chem. Eng. J. 379 (2020).
588 https://doi.org/10.1016/j.cej.2019.122320.

589 [55] H. Wu, L. Gong, X. Zhang, F. He, Z. Li, Bifunctional porous polyethyleneimine-grafted
590 lignin microspheres for efficient adsorption of 2,4-dichlorophenoxyacetic acid over a
591 wide pH range and controlled release, Chem. Eng. J. 411 (2021) 128539.
592 https://doi.org/10.1016/j.cej.2021.128539.

593 [56] G. Cruz González, C. Julcour, H. Chaumat, U. Jáuregui-Haza, H. Delmas, Degradation of
594 2,4-dichlorophenoxyacetic acid by photolysis and photo-Fenton oxidation, J. Environ.
595 Chem. Eng. 6 (2018) 874–882. https://doi.org/10.1016/j.jece.2017.12.049.

596 [57] A.C. Lua, T. Yang, Effect of activation temperature on the textural and chemical
597 properties of potassium hydroxide activated carbon prepared from the pistachio-nut
598 shell, J. Colloid Interface Sci. 274 (2004) 594–601.
599 https://doi.org/10.1016/j.jcis.2003.10.001.

600 [58] C. Bouchelta, M.S. Medjram, O. Bertrand, J.P. Bellat, Preparation and characterization
601 of activated carbon from date stones by physical activation with steam, J. Anal. Appl.
602 Pyrolysis. 82 (2008) 70–77. https://doi.org/10.1016/j.jaap.2007.12.009.

603 [59] X. Li, S. Deng, H. Fu, Inhibition of the corrosion of steel in HCl, H2SO4 solutions by
604 bamboo leaf extract, Corros. Sci. 62 (2012) 163–175.

https://doi.org/10.1016/j.corsci.2012.05.008.

[60] A.C. Lua, T. Yang, J. Guo, Effects of pyrolysis conditions on the properties of activated carbons prepared from pistachio-nut shells, J. Anal. Appl. Pyrolysis. 72 (2004) 279–287. https://doi.org/10.1016/j.jaap.2004.08.001.

[61] A.T. Mohd Din, B.H. Hameed, A.L. Ahmad, Batch adsorption of phenol onto physiochemical-activated coconut shell, J. Hazard. Mater. 161 (2009) 1522–1529. https://doi.org/10.1016/j.jhazmat.2008.05.009.

[62] F. Dhaouadi, L. Sellaoui, S. Taamalli, F. Louis, A. El, M. Badawi, J. Georgin, D.S.P. Franco, L.F.O. Silva, Enhanced adsorption of ketoprofen and 2 , 4-dichlorophenoxyactic acid on Physalis peruviana fruit residue functionalized with H 2 SO 4 : Adsorption properties and statistical physics modeling Adri a, 445 (2022). https://doi.org/10.1016/j.cej.2022.136773.

[63] J. Georgin, F.C. Drumm, P. Grassi, D. Franco, D. Allasia, G.L. Dotto, F. Caroline, D. Patrícia, G. Dison, F. Guilherme, L. Dotto, Potential of Araucaria angustifolia bark as adsorbent to remove Gentian Violet dye from aqueous effluents, Water Sci. Technol. 78 (2018) 1693–1703. https://doi.org/10.2166/wst.2018.448.

[64] J. Georgin, D.S.P. Franco, P. Grassi, D. Tonato, D.G.A. Piccilli, L. Meili, G.L. Dotto, Potential of Cedrella fissilis bark as an adsorbent for the removal of red 97 dye from aqueous effluents, Environ. Sci. Pollut. Res. 26 (2019) 19207–19219. https://doi.org/10.1007/s11356-019-05321-9.

[65] P.T. Hernandes, M.L.S.S. Oliveira, J. Georgin, D.S.P.P. Franco, D. Allasia, G.L. Dotto, Adsorptive decontamination of wastewater containing methylene blue dye using golden trumpet tree bark (Handroanthus albus), Environ. Sci. Pollut. Res. 26 (2019) 31924–31933. https://doi.org/10.1007/s11356-019-06353-x.

[66] P. Grassi, F.C. Drumm, J. Georgin, D.S.P. Franco, G.L. Dotto, E.L. Foletto, S.L. Jahn, Application of Cordia trichotoma sawdust as an effective biosorbent for removal of crystal violet from aqueous solution in the batch system and fixed-bed column, Environ. Sci. Pollut. Res. 28 (2021) 6771–6783. https://doi.org/10.1007/s11356-020-11005-6.

[67] J. Georgin, K. da Boit Martinello, D.S.P. Franco, M.S. Netto, D.G.A. Piccilli, E.L. Foletto, L.F.O. Silva, G.L. Dotto, Efficient removal of naproxen from aqueous solution by highly porous activated carbon produced from Grapetree (Plinia cauliflora) fruit peels, J. Environ. Chem. Eng. 9 (2021). https://doi.org/10.1016/j.jece.2021.106820.

[68] J. Georgin, D.S.P.P. Franco, M.S. Netto, D. Allasia, M.L.S.S. Oliveira, G.L. Dotto, Treatment of water containing methylene by biosorption using Brazilian berry seeds (Eugenia uniflora), Environ. Sci. Pollut. Res. 27 (2020) 20831–20843. https://doi.org/10.1007/s11356-020-08496-8.

[69] D.S.P. Franco, J. Georgin, F.C. Drumm, M.S. Netto, D. Allasia, M.L.S. Oliveira, G.L. Dotto, Araticum (Annona crassiflora) seed powder (ASP) for the treatment of colored effluents by biosorption, Environ. Sci. Pollut. Res. 27 (2020) 11184–11194. https://doi.org/10.1007/s11356-019-07490-z.

[70] Y.L. Salomón, J. Georgin, D.S.P. Franco, M.S. Netto, D.G.A. Piccilli, E.L. Foletto, D. Pinto,

M.L.S. Oliveira, G.L. Dotto, Adsorption of atrazine herbicide from water by diospyros kaki fruit waste activated carbon, J. Mol. Liq. 347 (2022) 117990. https://doi.org/10.1016/j.molliq.2021.117990.

[71] Y. Vieira, C. Schnorr, A.C. Piazzi, M.S. Netto, W.M. Piccini, D.S.P. Franco, E.S. Mallmann, J. Georgin, L.F.O. Silva, G.L. Dotto, An advanced combination of density functional theory simulations and statistical physics modeling in the unveiling and prediction of adsorption mechanisms of 2,4-D pesticide to activated carbon, J. Mol. Liq. 361 (2022) 119639. https://doi.org/10.1016/j.molliq.2022.119639.

[72] Y.L. de O. Salomón, J. Georgin, G.S. dos Reis, É.C. Lima, M.L.S. Oliveira, D.S.P. Franco, M.S. Netto, D. Allasia, G.L. Dotto, Utilization of Pacara Earpod tree (Enterolobium contortisilquum) and Ironwood (Caesalpinia leiostachya) seeds as low-cost biosorbents for removal of basic fuchsin, Environ. Sci. Pollut. Res. 27 (2020) 33307–33320. https://doi.org/10.1007/s11356-020-09471-z.

[73] D.S.P. Franco, J. Georgin, M.S. Netto, D. Allasia, M.L.S. Oliveira, E.L. Foletto, G.L. Dotto, Highly effective adsorption of synthetic phenol effluent by a novel activated carbon prepared from fruit wastes of the Ceiba speciosa forest species, J. Environ. Chem. Eng. 9 (2021) 105927. https://doi.org/10.1016/j.jece.2021.105927.

[74] J.S. Lazarotto, C. Schnorr, J. Georgin, D.S.P. Franco, M.S. Netto, D.G.A. Piccilli, L.F.O. Silva, C.R.B. Rhoden, G.L. Dotto, Microporous activated carbon from the fruits of the invasive species Hovenia dulcis to remove the herbicide atrazine from waters, J. Mol. Liq. 364 (2022) 120014. https://doi.org/10.1016/j.molliq.2022.120014.

[75] I. Ali, Z.A. Alothman, A. Alwarthan, Uptake of propranolol on ionic liquid iron nanocomposite adsorbent: Kinetic, thermodynamics and mechanism of adsorption, Elsevier B.V, 2017. https://doi.org/10.1016/j.molliq.2017.04.028.

[76] M. del Mar Orta, J. Martín, S. Medina-Carrasco, J.L. Santos, I. Aparicio, E. Alonso, Adsorption of propranolol onto montmorillonite: Kinetic, isotherm and pH studies, Appl. Clay Sci. 173 (2019) 107–114. https://doi.org/10.1016/j.clay.2019.03.015.

[77] R. George, S. Sugunan, Kinetics of adsorption of lipase onto different mesoporous materials: Evaluation of Avrami model and leaching studies, J. Mol. Catal. B Enzym. 105 (2014) 26–32. https://doi.org/10.1016/j.molcatb.2014.03.008.

[78] M. Songolzadeh, M. Soleimani, M. Takht Ravanchi, Using modified Avrami kinetic and two-component isotherm equation for modeling of CO2/N2 adsorption over a 13X zeolite bed, J. Nat. Gas Sci. Eng. 27 (2015) 831–841. https://doi.org/10.1016/j.jngse.2015.09.029.

[79] B. Mehdi, H. Belkacemi, D. Brahmi-Ingrachen, L.A. Braham, L. Muhr, Study of nickel adsorption on NaCl-modified natural zeolite using response surface methodology and kinetics modeling, Groundw. Sustain. Dev. 17 (2022) 100757. https://doi.org/10.1016/j.gsd.2022.100757.

[80] X. Zhang, L. Cao, W. Xiang, Y. Xu, B. Gao, Preparation and evaluation of fine-tuned micropore biochar by lignin impregnation for CO2 and VOCs adsorption, Sep. Purif. Technol. 295 (2022) 121295. https://doi.org/10.1016/j.seppur.2022.121295.

[81] J. Martín, M. del M. Orta, S. Medina-Carrasco, J.L. Santos, I. Aparicio, E. Alonso, Removal of priority and emerging pollutants from aqueous media by adsorption onto synthetic organo-funtionalized high-charge swelling micas, Environ. Res. 164 (2018) 488–494. https://doi.org/10.1016/j.envres.2018.03.037.

[82] N.K. Haro, P. Del Vecchio, N.R. Marcilio, L.A. Féris, Removal of atenolol by adsorption – Study of kinetics and equilibrium, J. Clean. Prod. 154 (2017) 214–219. https://doi.org/10.1016/j.jclepro.2017.03.217.

[83] G.Z. Kyzas, A. Koltsakidou, S.G. Nanaki, D.N. Bikiaris, D.A. Lambropoulou, Removal of beta-blockers from aqueous media by adsorption onto graphene oxide, Sci. Total Environ. 537 (2015) 411–420. https://doi.org/10.1016/j.scitotenv.2015.07.144.

[84] C.H. Giles, T.H. MacEwan, S.N. Nakhwa, D. Smith, Studies in Adsorption. Part XI.* A System, J. Chem. Soc. 846 (1960) 3973–3993.

[85] A. Bonilla-Petriciolet, D.I. Mendoza-Castillo, G.L. Dotto, C.J. Duran-Valle, I.T. De Aguascalientes, Adsorption in Water Treatment, Elsevier Inc., 2019. https://doi.org/10.1016/B978-0-12-409547-2.14390-2.

[86] C.J. Geankoplis, Transport Processes and Unit Operations, Prentice-Hall Int. (1993) 1–937. http://books.google.com/books?id=i9-TQgAACAAJ&pgis=1.

[87] C.R. Wilke, P. Chang, Correlation of diffusion coefficients in dilute solutions, AIChE J. 1 (1955) 264–270. https://doi.org/10.1002/aic.690010222.

[88] F. Wang, X. Ren, H. Sun, L. Ma, H. Zhu, J. Xu, Sorption of polychlorinated biphenyls onto biochars derived from corn straw and the effect of propranolol, Bioresour. Technol. 219 (2016) 458–465. https://doi.org/10.1016/j.biortech.2016.08.006.

[89] G.R. Paixão, N.G. Camparotto, G. de V. Brião, R. de L. Oliveira, J.C. Colmenares, P. Prediger, M.G.A. Vieira, Synthesis of mesoporous P-doped carbon and its application in propranolol drug removal: Characterization, kinetics and isothermal studies, Chem. Eng. Res. Des. 187 (2022) 225–239. https://doi.org/10.1016/j.cherd.2022.09.009.

[90] F. Feizi, A.K. Sarmah, R. Rangsivek, K. Gobindlal, Adsorptive removal of propranolol under fixed-bed column using magnetic tyre char: Effects of wastewater effluent organic matter and ball milling, Environ. Pollut. 305 (2022) 119283. https://doi.org/10.1016/j.envpol.2022.119283.

List of Figures

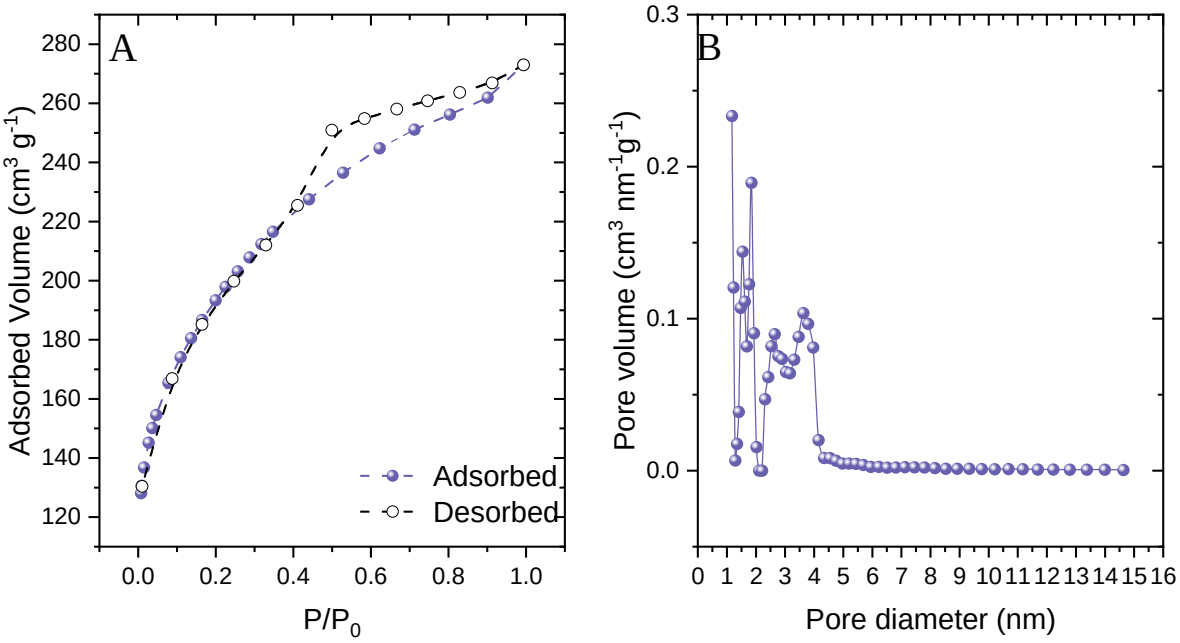

Fig. 1. N_2 adsorption-desorption isotherms (a) and desorption pore size distribution (b).

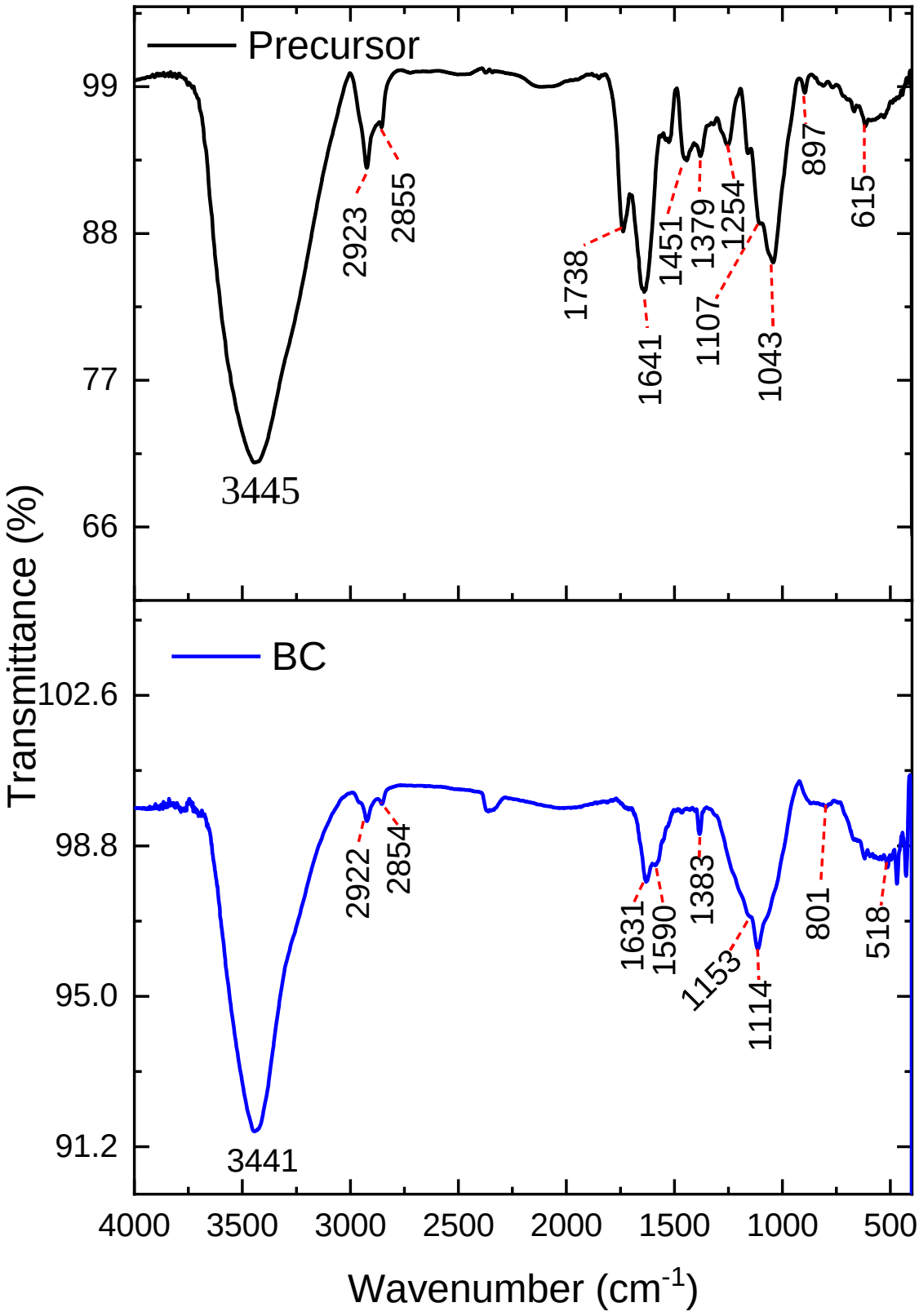

Fig. 2. FT-IR spectra precursor and BC.

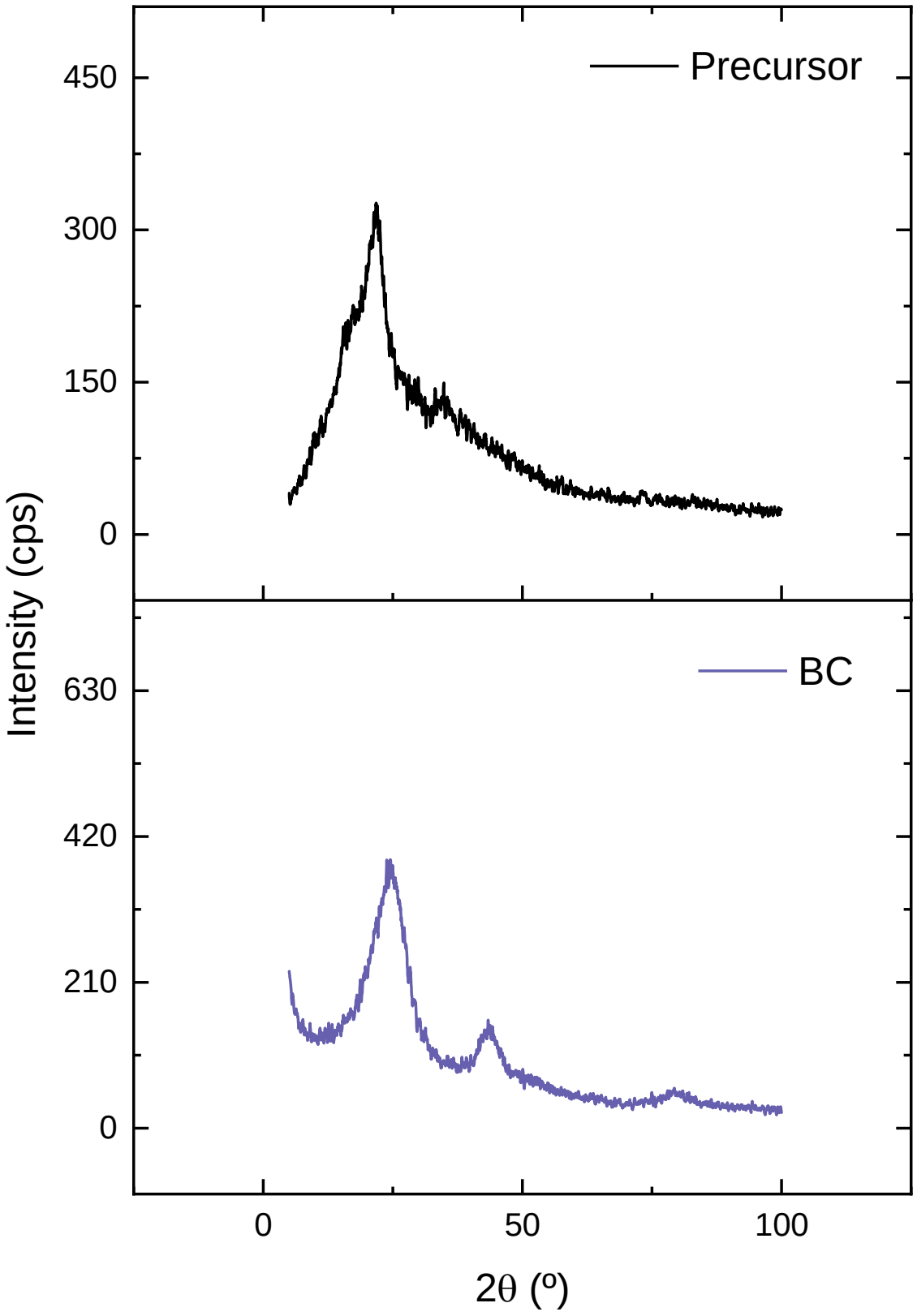

733

734 Fig. 3. XRD patterns for precursor and BC.

735

736

737 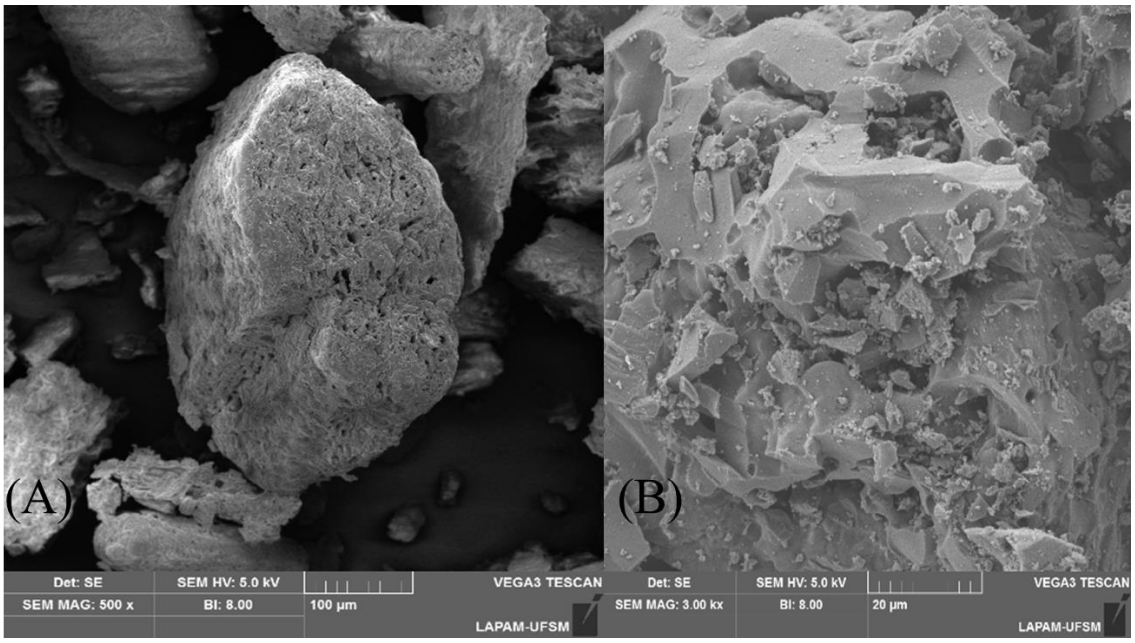

738 Fig. 4. SEM images of precursor material (A) and activated biochar (B).

739

740

741

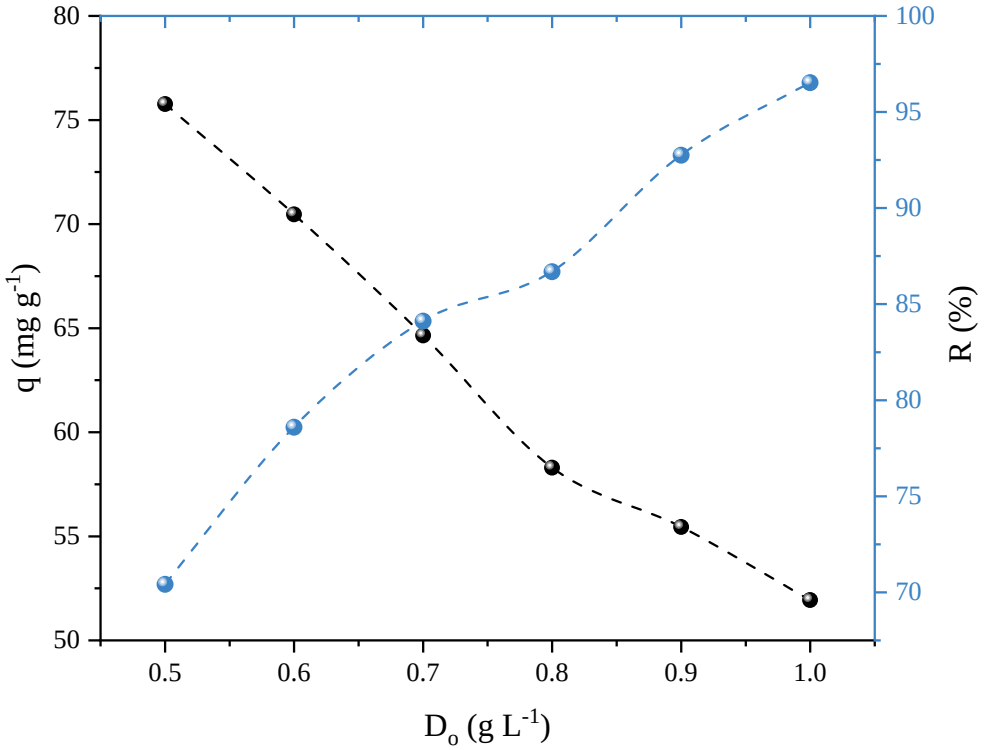

742

743 Fig.5. Biochar adsorbent dosage on PROP uptake. Conditions: C_0 = 25 mg L^{-1}, adsorbate volume 50 mL,

744 natural solution pH, t = 120 min, 298 K.

745

746

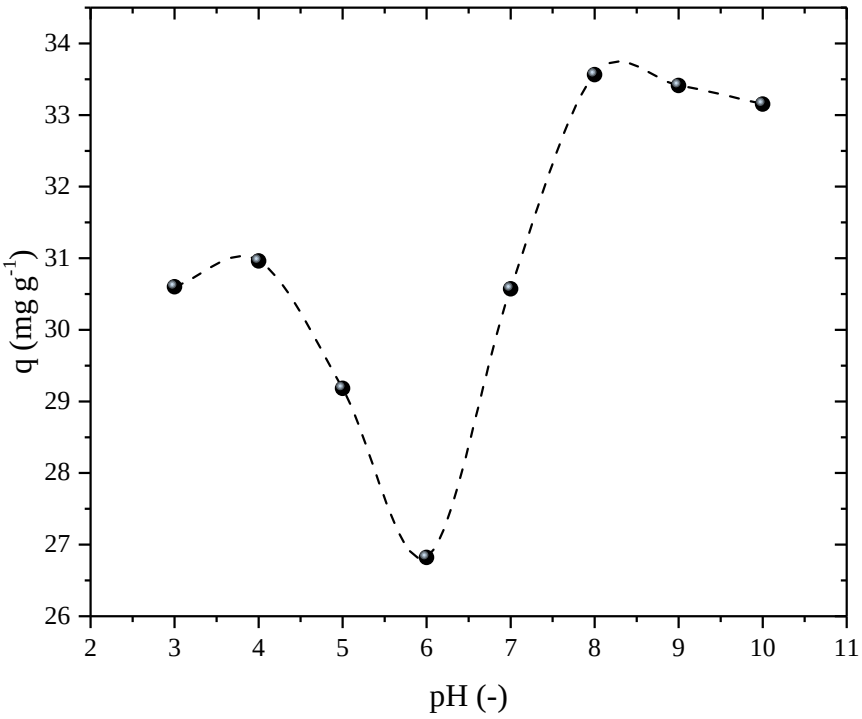

747

748 Fig.6. Effect of pH on PROP uptake. Conditions: adsorbate solution 50 mL, C_0 = 25 mg L^{-1}, adsorbent
749 dosage 0.7 g L^{-1}, contact time 120 min, 298 K.

750

751

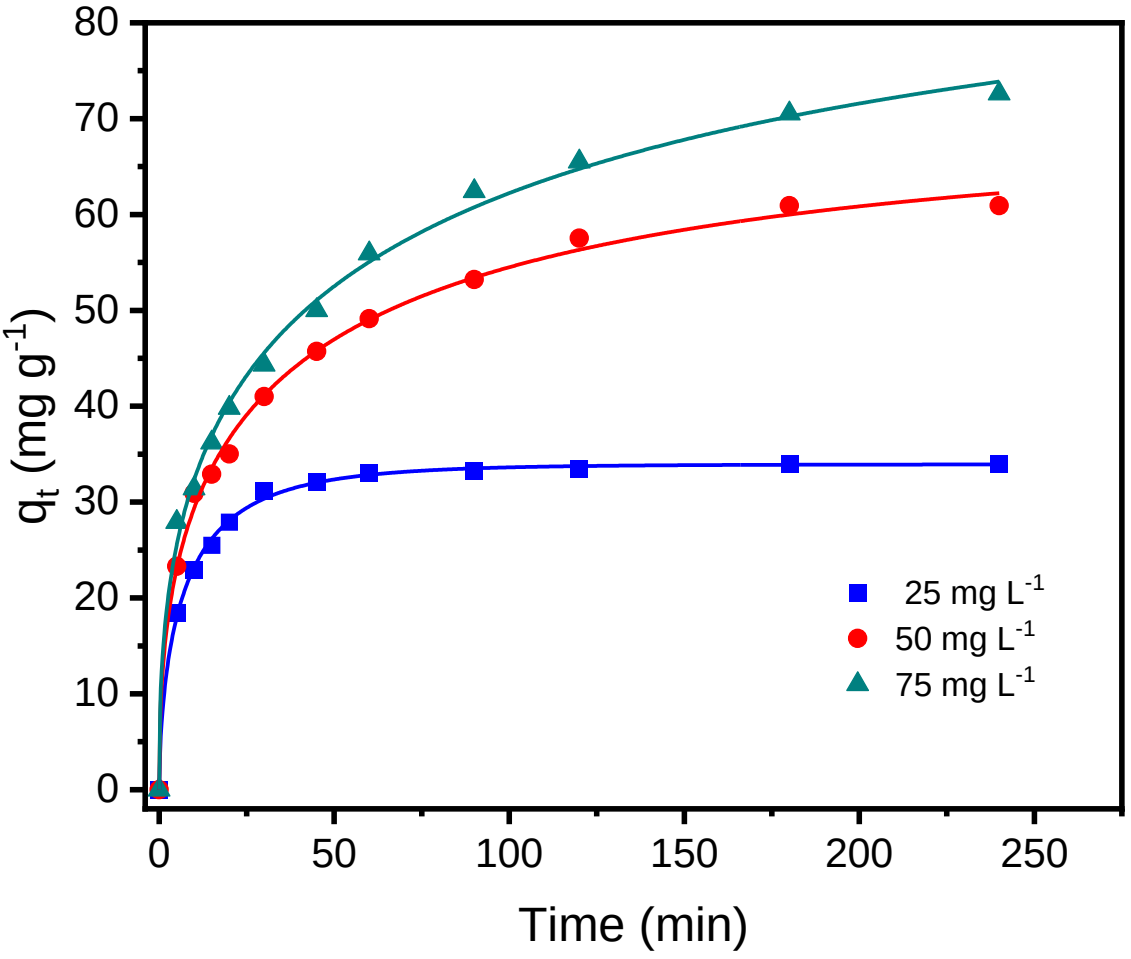

Fig. 7. Avrami fraction order kinetic model for the uptake of PROP onto activated biochar. Conditions: adsorbent dosage 0.7 g L^{-1}, initial pH = 8, adsorbent volume 25 mL, initial PROP concentration 25 mg L^{-1}.

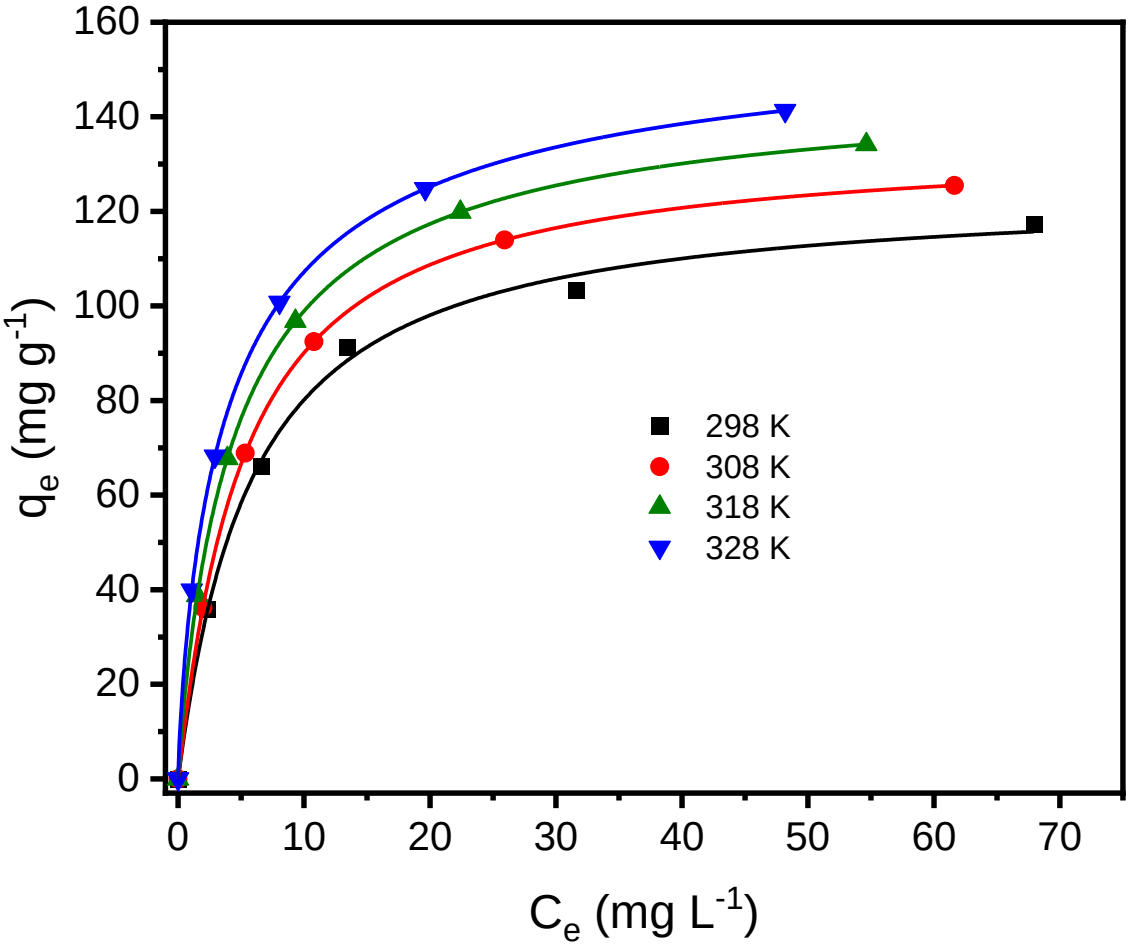

Fig.8. Liu equilibrium curves for the uptake of PROP on activated biochar at different temperatures. Conditions: initial PROP pH 8, adsorbent dosage 0.7 g L^{-1}, contact time 300 min.

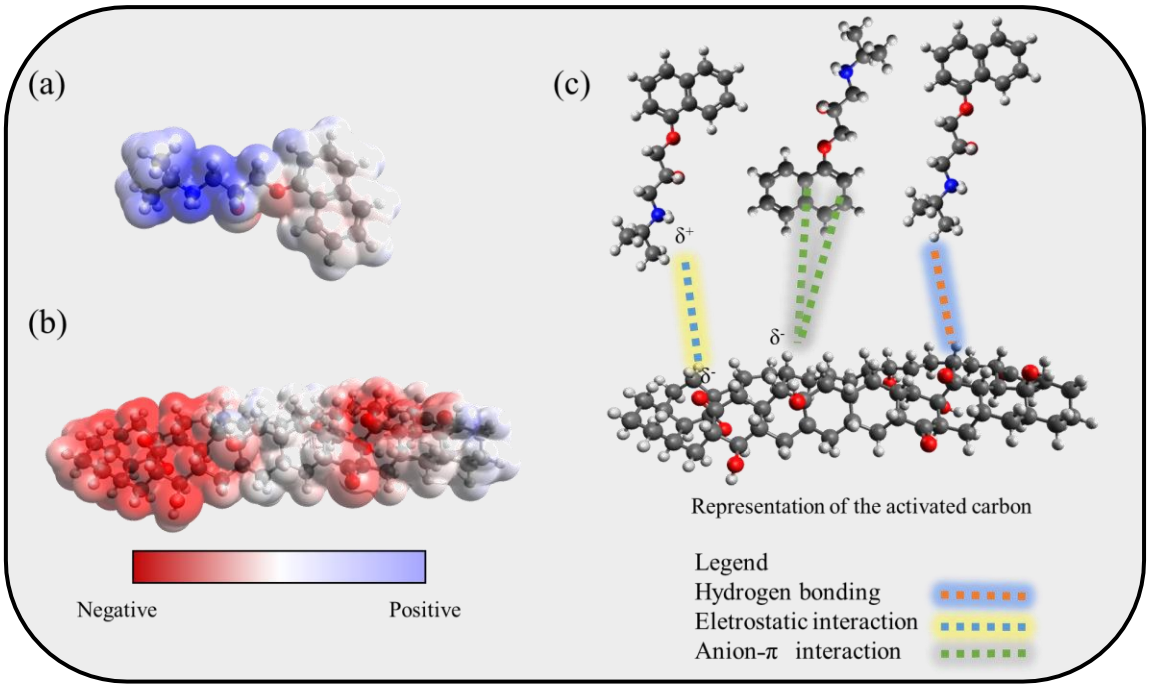

766

767 Fig.9. Proposed adsorption mechanism of PROP onto the adsorbent

768

769

770